Environmental Science and Ecotechnology 12 (2022) 100200

Contents lists available at ScienceDirect

Environmental Science and Ecotechnology

journal homepage: www.journals.elsevier.com/environmental-science-and-ecotechnology/

Original Research

# Vertically-resolved indoor measurements of air pollution during Chinese cooking

Shuxiu Zheng [a], Huizhong Shen [b, c, *], Guofeng Shen [a], Yilin Chen [b, c], Jianmin Ma [a], Hefa Cheng [a], Shu Tao [a, b, c]

[a] College of Urban and Environmental Sciences, Laboratory for Earth Surface Processes, Sino-French Institute for Earth System Science, Peking University, Beijing, 100871, China
[b] School of Environmental Science and Engineering, Southern University of Science and Technology, Shenzhen, 518055, China
[c] Guangdong Provincial Observation and Research Station for Coastal Atmosphere and Climate of the Greater Bay Area, Southern University of Science and Technology, Shenzhen, 518055, China

ARTICLE INFO

*Article history:*
Received 22 March 2022
Received in revised form
24 June 2022
Accepted 28 June 2022

*Keywords:*
Indoor air pollution
Chinese cooking
Vertical distribution
Particulate matter

ABSTRACT

Chinese cooking features several unique processes, e.g., stir-frying and pan-frying, which represent important sources of household air pollution. However, factors affecting household air pollution and the vertical variations of indoor pollutants during Chinese cooking are less clear. Here, using low-cost sensors with high time resolutions, we measured concentrations of five gas species and particulate matter (PM) in three different sizes at multiple heights in a kitchen during eighteen different Chinese cooking events. We found indoor gas species were elevated by 21%–106% during cooking, compared to the background, and PMs were elevated by 44%–159%. Vertically, the pollutants concentrations were highly variable during cooking periods. Gas species generally showed a monotonic increase with height, while PMs changed more diversely depending on the cooking activity's intensity. Intense cooking, e.g., stir-frying, pan-frying, or cooking on high heat, tended to shoot PMs to the upper layers, while moderate ones left PMs within the breathing zone. Individuals with different heights would be subject to different levels of household air pollution exposure during cooking. The high vertical variability challenges the current indoor standard that presumes a uniform pollution level within the breathing zone and thus has important implications for public health and policy making.



## 1. Introduction

Chinese residents are subject to severe exposure to household air pollution [1–4], which is associated with adverse health outcomes due primarily to direct exposure to air pollutants released from cooking and heating indoors [5]. In 2019, approximately 360,000 premature deaths in China were attributed to household air pollution, ranking the third among all environmental risk factors (following ambient particulate matter and non-optimal temperature) [6]. Previous studies demonstrated that cooking is one of the predominant sources of household air pollution [7]. In rural areas, the effects of cooking on household air pollution exposure, especially for rural residents who use solid fuels (e.g., coal and biomass fuels), have been widely studied [5,8–14]. For the urban counterpart, however, the role of cooking in household air pollution is less clear.

China's urban population is growing rapidly [15]. In urban households, natural gas is widely used for cooking [16]. According to the market research of China's urban gas industry, the popularity rate of gas fuel in Chinese urban areas reached 97.87% in early 2020, and the natural gas accounts for more than 70% of the total gas fuel [17]. In Beijing, 14.76 million people used natural gas as residential energy resources in 2020, accounting for 65% of the permanent population [17]. Combustion of natural gas releases a variety of greenhouse gases and air pollutants, such as carbon dioxide ($CO_2$), methane ($CH_4$), formaldehyde (HCHO), other volatile organic compounds (VOCs), carbon monoxide (CO), and particulate matter (PM), through combustion processes or gas leakage [18–21]. Chinese cooking features diversified cooking techniques (e.g., pan-

* Corresponding author. School of Environmental Science and Engineering, Southern University of Science and Technology, Shenzhen, 518055, China.
*E-mail address:* shenhz@sustech.edu.cn (H. Shen).

https://doi.org/10.1016/j.ese.2022.100200

frying and stir-frying) and ingredients/flavors (e.g., aromatic flavours), which may represent additional sources of air pollutants [22]. Several studies have characterized the indoor levels of these gas species and PM generated during cooking fueled by natural gas [23–26], but only a few focus on Chinese cooking [27–32]. Ardeh et al., for example, identified the use of natural gas as the main cause of the occurrences of substantial sharp spikes in observed indoor concentrations of formaldehyde and CO [20]. See et al. found that $PM_{2.5}$ concentrations during Chinese cooking with a gas stove were on average more than ten times higher than those during non-cooking periods [27]. Similar results were reported by Wallace et al. through long-term indoor measurements of size-resolved PM numbers [25]. Lai et al. showed that oil fumes splashed during stir-frying and deep-frying (two typical techniques of Chinese cooking) contributed to household air pollution in addition to the combustion of cooking fuels [22]. Pollutants concentrations during cooking vary with cooking duration, height, ventilation condition, cooking technique (e.g., boil, stir-fry, grilling, etc.), temperature, type of food (e.g., fatty food, vegetables, etc.), oil (e.g., olive oil, peanut oil, sunflower oil, etc.), fuel (e.g., natural gas, liquefied petroleum gas, electricity, etc.), etc [23,27]. Despite some past studies addressing parts of the influential factors [33,34], there is a lack of comprehensive assessment on how all these factors affect urban indoor air quality during Chinese cooking.

The indoor air quality standard in China adopts a fixed sampling height within the "breathing zone" (0.5–1.5 m above the floor for Chinese people) [35], presuming that concentrations within this zone are uniform. However, the vertical variations can be substantial because of cooking-induced strong convection in the indoor micro-environment [36,37]. Such variations in pollutants concentrations play an important role in the actual exposure of individuals [38,39]. Knowledge of the vertical variations during cooking thus have significant policy and health importance but is by far not clear.

In this study, we used photoacoustic gas monitors and low-cost PM sensors, which cost about 44 dollars each, to conduct continuous measurements of five gas species and PM in three sizes in a typical Chinese urban apartment that uses natural gas stove for cooking. We carried out different cooking activities associated with varying ventilation conditions, cooking techniques, temperatures, and types of food and ingredients. We measured concentrations at different heights during these cooking events, whereby the factors and vertical distributions of indoor gas and PM concentrations during Chinese cooking were characterized.

## 2. Methods

### 2.1. Experimental design

The experiment was conducted in the kitchen of a typical apartment (size, 88 $m^2$) in Beijing, China, on March 25th, 2020. The residential area is located in Haidian District situated in northwestern Beijing and is surrounded by university campuses such as Peking University. There were no heavy industrial sources nearby. There was only one window facing west in the kitchen equipped with a ventilator, and the experiment kitchen with one window, one ventilator, and one natural gas stove was typical for residents in Beijing [8]. A ventilator (ROBAM, CXW185-3012B) was used to remove some of the air pollutants produced during cooking in the kitchen. The floor plan is shown in Fig. S1. A natural gas range (ROBAM, JZ(Y/T/R)2-9G62) was used for cooking during the experiment (Fig. S1). The starting and ending times of each cooking event, the type of cooking activity (boiling water, scrambling eggs, or stir-frying), the ventilator's state (on-strong, on-weak, or off), the heating level (low, medium-low, medium, or high), and the heating burners (left or right, the cooktop was installed at 80 cm above the floor) during each cooking event, are shown in Table 1. Specifically, seven water-boiling activities with the kitchen ventilator off were conducted in the morning. During the first water-boiling activity, the left heating burner was lighted twice to test the impact of lighting. The following six water-boiling activities corresponded to six different combinations of the two burners (left or right) with three heating levels (low, medium, or high), while each time, the burner was lighted only once. This set of experiments was designed to test the contribution of fuel combustion to household air pollution and the impacts of heating levels on household air pollution when the ventilator was off. At noon, three cooking activities with ingredients were conducted in sequence at 10- to 20-min intervals, including heating garlic sprouts on the left burner with the kitchen ventilator on and scrambling eggs on the right burner twice with the kitchen ventilator on and off, respectively. In the afternoon, another six water boiling activities were conducted to test the impacts of heating levels on household air pollution when the ventilator was on. The water got boiled during all the water boiling events. Following these water boiling activities, a complete cooking of multiple ingredients (Act. No. 19 listed in Table 1) was conducted under the high heating level in two steps, i.e., pan-frying pepper and onion and then stir-frying cabbage, with the ventilator on. The same frying cooking event (Act. No. 20 listed in Table 1) was then repeated but with the ventilator off. The cooking techniques in the experiment, i.e., water boiling, condiments heating, scrambling, stir-frying, and pan-frying, were typical in northern China [27,28,30,32,40].

The window in the kitchen was closed during cooking. To ensure a background pollution level at the beginning of each cooking activity, we turned on the ventilator (at the on-strong state) and kept the window open during the intervals between cooking activities. Each interval lasted for at least 15 min. After the last cooking activity (i.e., stir-frying cabbage after pan-frying pepper and onion with the ventilator off), we kept the window closed and the ventilator off to investigate how long the impact of cooking on household air pollution would persist in the absence of significant ventilation.

### 2.2. Measurements

The floor plan of the apartment, the location of the indoor site, and the layout of the monitoring equipment are shown in Fig. S1. A photoacoustic gas monitor (INNOVA 1512, LumaSense Tech. A/S, Ballerup, Denmark) with a six-channel multipoint sampler (INNOVA 1409, LumaSense Tech. A/S, Ballerup, Denmark) was used to monitor five gas species, including formaldehyde, $CO_2$, CO, total VOCs (TVOCs), and methane. The concentration of TVOCs here was identified as the toluene-equivalent total concentration. The monitor was compensated for temperature, pressure fluctuations, water vapor interference, and interferences from other known gases in the sample air in advance so that the monitor could automatically correct the influence of temperature, pressure, water vapor, and other known gases on the concentrations of detected gas. During the calibration, standard high purity dry nitrogen (the purity is higher than 99.9999%) was used to determine the zero of each gas, and then we used standard gas of higher concentration (13.2 mg $m^{-3}$ for formaldehyde, 1400 mg $m^{-3}$ for $CO_2$, 50 mg $m^{-3}$ for CO, 75.8 mg $m^{-3}$ for toluene, and 202 mg $m^{-3}$ for $CH_4$) to determine the conversion coefficients of signal strength and concentrations of each gas species, considering the signal strength varied linearly with the concentrations of specific gas species according to previous studies [41]. The photoacoustic infrared technology was employed to detect the concentration of different gas species. When the sample gas of interest is exposed to a specific

**Table 1**
**Summary of the indoor monitoring campaign.** The starting and ending times of each cooking event, the type of cooking activity, the ventilator's state, the heating level, and the burner locations of each cooking activity were listed in the table. The ventilator was either kept on or off for each cooking event. The state of the ventilator would not change during cooking. The window was kept closed during all the cooking events, and it was opened for at least 10 min during the intervals of two cooking events such that the impacts of the previous cooking event on the proceeding one could be minimized. And during the intervals, the ventilator was turned on to the on-strong state.

| Activity No. | Starting time | Ending time | Activity | Ventilator | Burner | Heat |
|---|---|---|---|---|---|---|
| 1 | 7:50 | 7:55 | Ventilating | On-strong | | |
| 2 | 7:55 | 8:00 | Two people preparing in the kitchen | On-strong | | |
| 3 | 8:25 | 8:28 | Boiling water (strike the light twice) | Off | Left | Low |
| 4 | 8:49 | 8:52 | Boiling water | Off | Right | Low |
| 5 | 9:15 | 9:20 | Boiling water | Off | Left | Low |
| 6 | 9:39 | 9:44 | Boiling water | Off | Right | Medium |
| 7 | 10:06 | 10:11 | Boiling water | Off | Left | Medium |
| 8 | 10:30 | 10:35 | Boiling water | Off | Right | High |
| 9 | 10:55 | 11:06 | Boiling water | Off | Left | High |
| 10 | 11:22 | 11:28 | Heating the garlic sprouts | On-strong | Left | Medium-low |
| 11 | 11:40 | 11:45 | Scrambling eggs | On-strong | Right | Medium-low |
| 12 | 12:04 | 12:09 | Scrambling eggs | Off | Right | Medium-low |
| 13 | 12:59 | 13:04 | Boiling water | Off | Left | Low |
| 14 | 13:46 | 13:51 | Boiling water | On-weak | Left | Low |
| 15 | 14:24 | 14:29 | Boiling water | On-weak | Right | Low |
| 16 | 15:26 | 15:34 | Boiling water | On-weak | Right | Medium |
| 17 | 16:12 | 16:17 | Boiling water | On-weak | Left | High |
| 18 | 16:56 | 17:01 | Boiling water | On-weak | Right | High |
| 19 | 18:39 | 18:46 | Stir-frying the cabbage after pan-frying the pepper and onion | On-strong | Left | High |
| 20 | 19:17 | 19:26 | Stir-frying the cabbage after pan-frying the pepper and onion | Off | Left | High |

wavelength of infrared light (the central wavelength of the five gas species above is 3.6, 4.4, 4.7, 3.4, and 8.0 μm, respectively), it will absorb an amount of infrared light proportional to its concentration, and an audible pulse caused by the extra pressure of the activated gas molecular can be detected by the extremely sensitive monitor photoacoustic gas monitor. The detection limits of formaldehyde, $CO_2$, CO, TVOCs, and methane are 0.04, 8.75, 0.2, 0.05, and 0.4 mg $m^{-3}$, respectively, with acceptable uncertainties (Table S21). The six channels of the multipoint sampler were set at six different heights (i.e., 19, 40, 78, 119, 147, and 199 cm) to obtain vertical information (Fig. S1). Three heights (78, 119, and 147 cm) were set within the breathing zone (0.5–1.5 m), which was the exposure height of the majority of the population. Two heights (19 and 40 cm) were set below 0.5 m to monitor the concentration fluctuations above the floor, and one height (199 cm) was set beneath the roof to monitor the concentrations of gas species at a higher height. Gas flows from the six channels were measured alternately by the same detector with a 1-min time lag between adjacent channels. The time resolution of each channel was thus 6 min. Given that there were slight differences between different channels, factor correction was performed to adjust the readings of the six channels by gathering the six channels at the same height and measuring the concentration synchronously. Details for the adjustment are provided in Supplementary Materials (Text S1 and Table S3).

Eleven customized online PM monitors were evenly spaced at 20–220 cm heights to provide detailed vertical variations of PM concentrations and, simultaneously, to ensure that the sensors didn't affect each other. There was a certain difference (1–2 cm for five heights) between the sampling heights of gas species and PM to ensure that the gas samplers wouldn't interfere with PM sensors when fixed. The PM monitors consisted of online particle counters (Green Built EnvMent., Beijing, China) and laser scattering sensors (Plantower PMS3003, Beijing, China) (Fig. S1). The particle sensors inverted the concentrations of particulate matter based on the scattering light intensity of particulate matter to the laser. Therefore, in principle, the water vapor does not affect the scattering unless the formation of liquid particles and growth of existing particles by heterogeneous nucleation occurs. The monitor is about the size of $3 \times 4 \times 5$ $cm^3$ (Fig. S1), with a fan working at a constant speed. When operating, there is a small local circulation around the fan, so surrounding air can enter the monitor through the air channel. The local circulation is much smaller than the distance between two adjacent monitors such that adjacent monitors wouldn't interact with each other. The online monitor coverts the unit from number density to mass density automatically. All the PM monitors were pre-calibrated by a hybrid ambient real-time particulate monitor (Model 5030 SHARP, Synchronized Hybrid Ambient, Real-time Particulate Monitor, Thermo Scientific). Detailed calibration processes and the calibration coefficients of the eleven monitors are provided in Supplementary Materials (Text S2 and Table S4). Both the PM sensors and the gas monitor were employed in previous studies to detect indoor air pollution, showing good agreement with reference monitoring systems and easier deployment compared to conventional monitoring systems [3,4,42].

### 2.3. Data analysis

RStudio (Version 1.2.5001) was used for descriptive statistic derivation, and the significance level was set at 0.01 for all statistical tests [43]. Cooking periods were defined as the periods when cooking was conducted. Non-cooking periods that represent the synchronous background concentration were defined as part of the intervals between two cooking activities after the window was opened for at least 10 min. Considering that we conducted strong ventilation during the intervals (two ventilators were turned on to the on-strong state, and the window was widely opened), the impacts of the proceeding cooking events on non-cooking periods should be minor after the 10-min ventilation. We further investigated the vertical transport of the gas species and PM during each cooking activity by comparing the "peak-time"—the time when the concentration of the pollutant reached its maximum during each cooking activity at different heights. We employed the hourly $PM_{2.5}$ concentration time series reported by Beijing municipal routine monitoring station at Wan Liu, the closest monitoring station to the experimental site, as the outdoor $PM_{2.5}$ concentration reference.

## 3. Results and discussion

### 3.1. Indoor concentrations of gas species and PM

The average concentrations of formaldehyde, $CO_2$, CO, TVOCs, and methane during the entire monitoring period (combining both cooking and non-cooking periods) were 0.31, 1862, 6.75, 3.69, and 6.60 mg $m^{-3}$, respectively. The levels of $CO_2$ and CO were around China's indoor air quality standards (1750 mg $m^{-3}$ for $CO_2$ and 10 mg $m^{-3}$ for CO), with $CO_2$ being 6% higher than the standard and CO being 34% lower [35]. The level of formaldehyde, on the other hand, was much higher than its indoor standard (0.1 mg $m^{-3}$) [35], exceeding by 210%, suggesting the presence of high levels of organic compounds during the experiment. For the other two gas species, methane is not on the list of the national indoor air quality standard nor in the WHO guidelines [44]; the concentration of TVOCs was operationally defined and was calibrated against toluene—the analytical method for TVOCs was different from that defined by the national indoor air quality standard, so they were not comparable. In addition, the health standards of TVOCs were not provided in WHO guidelines for indoor air quality [44].

The concentration frequency distributions of the five gas species (averaged vertically to reflect the mean levels of all layers) were right-skewed and leptokurtic (Fig. S2 and Table S5), meaning that the distributions had sharper and right-skewed peaks than corresponding normal distributions. In addition, according to Lilliefors tests ($p < 0.01$), the concentration frequency distributions were significantly different from normal distributions (Table S7). After a logarithmic transformation, the distributions of all species were still right-skewed and leptokurtic, mainly driven by several observed sharp concentration spikes (Table S7 and Fig. S2). Further investigation showed that these sharp spikes occurred in company with cooking events. As is shown in Fig. 1, the median levels of formaldehyde, $CO_2$, CO, TVOCs, and methane during cooking periods were 0.29, 2068.10, 6.84, 3.76, and 6.58 mg $m^{-3}$, respectively. The levels of $CO_2$ and CO were close to China's indoor air quality standards (1750 mg $m^{-3}$ for $CO_2$ and 10 mg $m^{-3}$ for CO), with $CO_2$ being 18% higher than the standard and CO being 32% lower. The level of formaldehyde, however, was well above its indoor standard (0.1 mg $m^{-3}$), exceeding by 190%. In addition, the median levels of formaldehyde, $CO_2$, CO, TVOCs, and methane during cooking periods were 35%, 52%, 181%, 47%, and 36% higher than those during non-cooking periods, and the differences in maximum levels were even larger. For example, the formaldehyde concentration reached 2.09 mg $m^{-3}$ during the cooking activities, 432% higher than the highest level observed during non-cooking periods (0.39 mg $m^{-3}$). T-tests showed that the concentrations of all gas species during cooking activities were statistically significantly higher than those during non-cooking periods ($p < 0.01$).

The average concentrations of $PM_1$, $PM_{2.5}$, and $PM_{10}$ were 29, 48, and 61 μg $m^{-3}$, respectively, during the experiment. The average $PM_{2.5}$ was 92% higher than the threshold limit value of 24-h $PM_{2.5}$ provided in WHO IAQ standards and guidelines (25 μg $m^{-3}$) (note that, currently, there is no indoor $PM_{2.5}$ standard in China) [46,47]. The average $PM_{10}$ was lower than both the Chinese indoor standard (150 μg $m^{-3}$) and 24-h Level-II ambient standard (150 μg $m^{-3}$), while exceeded the Level-I ambient standard (50 μg $m^{-3}$) by 22%. Like most gas species, the distributions of PM concentrations of individual sizes were right-skewed and leptokurtic both before and after logarithmic transformation (Fig. S3 and Table S6) and, therefore, significantly differed from normal distributions (Table S8) due to occurrences of high concentration spikes.

The median levels of $PM_1$, $PM_{2.5}$, and $PM_{10}$ during cooking periods were 37.8, 62.3, and 77.0 mg $m^{-3}$, respectively (Fig. 1). The median $PM_{2.5}$ concentration was about one and a half times beyond the threshold limit value of 24-h $PM_{2.5}$ (25 μg $m^{-3}$) provided in WHO IAQ standards and guidelines [47]. Similar to the gas species, elevated PM levels were found during cooking activities (*t*-test, $p < 0.01$) (Fig. 1), with the median concentrations of $PM_1$, $PM_{2.5}$, and $PM_{10}$ during cooking periods being 62%, 70%, and 68% higher, respectively, than those during non-cooking periods. The peak levels were 605%, 1241%, and 1534% higher, respectively, during cooking periods than those during non-cooking periods, which were more pronounced than the differences in gas species.

### 3.2. Vertical distributions

The vertically-resolved measurements revealed that the gas

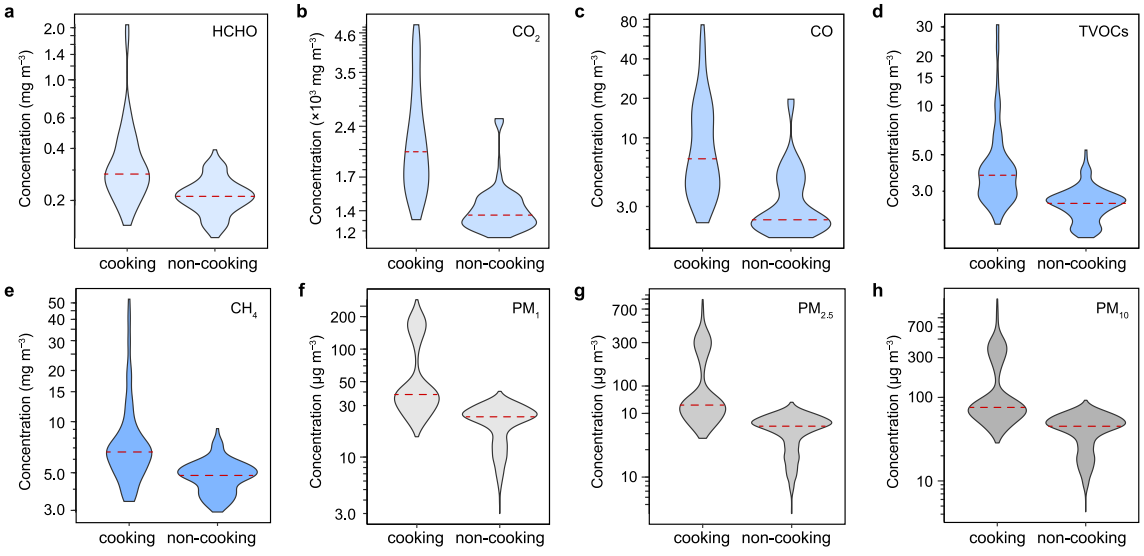


**Fig. 1.** Violin plots showing the probability density of the concentrations of five gas species, including formaldehyde (HCHO, **a**), carbon dioxide ($CO_2$, **b**), carbon monoxide (CO, **c**), total volatile organic carbon (TVOCs, **d**), and methane ($CH_4$, **e**), and three sizes of particulate matters ($PM_1$, $PM_{2.5}$, $PM_{10}$, **f**–**h**) at different heights during cooking and non-cooking periods. The probability density was estimated by the kernel density estimation method, a non-parametric method used to estimate an unknown probability density function through a kernel function [45]. To put it more vividly, the wider the violin body, the more concentrated the data. Y-axes are on the logarithmic scale. The median levels are marked by red dashed lines.

concentrations at higher heights were generally higher than those at lower heights during cooking periods (Fig. 2). The average concentrations at 199 cm, for example, were 74% (for $CO_2$) to 182% (for CO) higher than those at 78 cm during cooking periods. It should be noted that 199 and 78 cm were chosen here as two representative heights for discussion purposes, considering that 78 cm was the minimum sampling height within the breathing zone and concentrations at 199 cm were least correlated with the concentrations at 78 cm (shown in Table S20). T-test analyses showed that the ratios of the concentrations in the upper layer (199 cm) to those in the lower layer (78 cm) were significantly greater than 1 for formaldehyde, $CO_2$, CO, and methane during cooking periods ($p < 0.01$; for TVOCs, $p = 0.016$) (Table S9). A monotonic increase in concentration over height was evident for every layer above 40 cm and every gas species (Fig. 2). In contrast, vertical differences were not statistically significant during non-cooking periods (Fig. 2 and Table S10).

Concentration spikes were found during cooking periods in all layers but appeared at slightly different times. Spikes in the upper layers proceeded with those in the lower layers (Fig. S4). The time

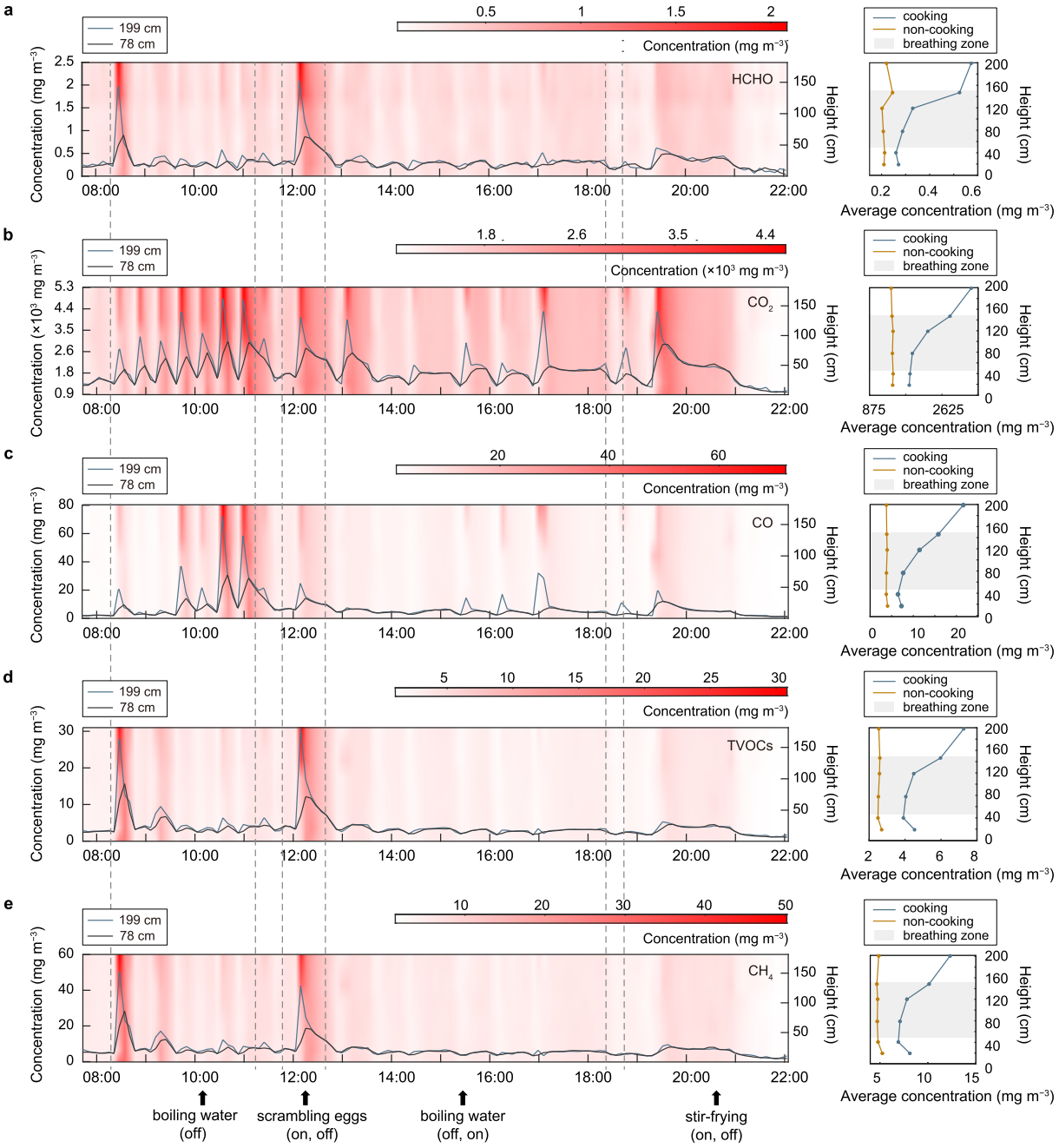


**Fig. 2. The temporal and vertical variations of indoor gas species.** Temporal and vertical variance of concentrations of five gas species, including formaldehyde (HCHO, **a**), carbon dioxide ($CO_2$, **b**), carbon monoxide (CO, **c**), total volatile organic carbon (TVOCs, **d**), and methane ($CH_4$, **e**), during the study period are shown on the left-side panel. The heights above the floor are shown on the right-y-axis. The darker the red color, the higher the concentration, as shown by the color bar above. The black and blue lines represent the concentrations (as shown on the left-y-axis) of gas species (mg $m^{-3}$) at 78 cm and 199 cm, respectively. The types of cooking events are marked by black arrows on the bottom of the left-side panel. The average concentrations of five gas species during both cooking and non-cooking period at different heights (right) (Table S19) are shown on the far-right side of each panel. The grey box shape represents the breathing zone of 0.5–1.5 m. The measurement was conducted in the kitchen, and the concentrations were derived from a photoacoustic gas monitor with a 6-min temporal resolution. The six detection heights were 19, 40, 78, 119, 147, and 199 cm above the floor, respectively.

lags between 199-cm and 78-cm heights were about 6 min, with the spikes at 199 cm happening first (Fig. 2). Thus, the gas species that were carried by the cooking-induced convection of hot air accumulated in the upper layers first and then spread downward to the lower layers.

As opposed to gas species, the vertical gradients of PM were not monotonic during cooking periods (Fig. 3). Higher heights did not necessarily show higher concentrations (Fig. 3). The analysis of variance (ANOVA) for PM during cooking (excluding the last two events associated with intense cooking, i.e., stir-frying the cabbage after pan-frying the pepper and onion with the ventilator on and off, respectively, Supplementary Text S4 for the analysis of variance method) showed significant difference among eleven heights ($p < 0.05$ for $PM_1$ and $PM_{2.5}$, $p < 0.01$ for $PM_{10}$). Subsequent Student-Newman-Keuls multi-comparison classified the eleven heights into five (for $PM_1$ and $PM_{2.5}$) or six (for $PM_{10}$) concentration groups (Fig. S5). For the three PM sizes, the 100-cm height showed the highest concentration consistently, and the 80-cm height came second (Fig. S5). Note that 80–100 cm was about the flame's height. Together with the other three heights, the five monitored heights located in the breathing zone (i.e., 60, 80, 100, 120, and 140 cm) were scattered in three or four different groups (Fig. S5), suggesting rather variable vertical profiles of PM within the breathing zone.

During the last two intense cooking events, consisting of stir- and pan-frying procedures and represented intense cooking, the highest PM levels were found in the upper layers (with height $\geq$140 cm) rather than at the 80-cm or 100-cm height (Figs. S6 and S7). For example, during the second last event, the three layers at the top (180, 200, and 220 cm) were associated with the highest PM levels among all layers (Fig. S6), which was very different from most of the previous events when PM levels in these three layers were among the lowest (Fig. S5). Similar results were found during the last event, with the heights of 140, 160, and 200 cm showing the highest PM levels (Fig. S7). Given that the last two events were the only two events involving stir- and pan-frying, the elevation of the upper-layer PM during these events was likely a result of these procedures, which are commonly conducted during Chinese cooking.

In addition to the last two events, observed elevation in upper-layer PM can be found in another three events, including heating garlic sprouts (Activity No. 10), scrambling eggs (No. 12), and boiling water on high heat (No. 18), respectively, which were all associated

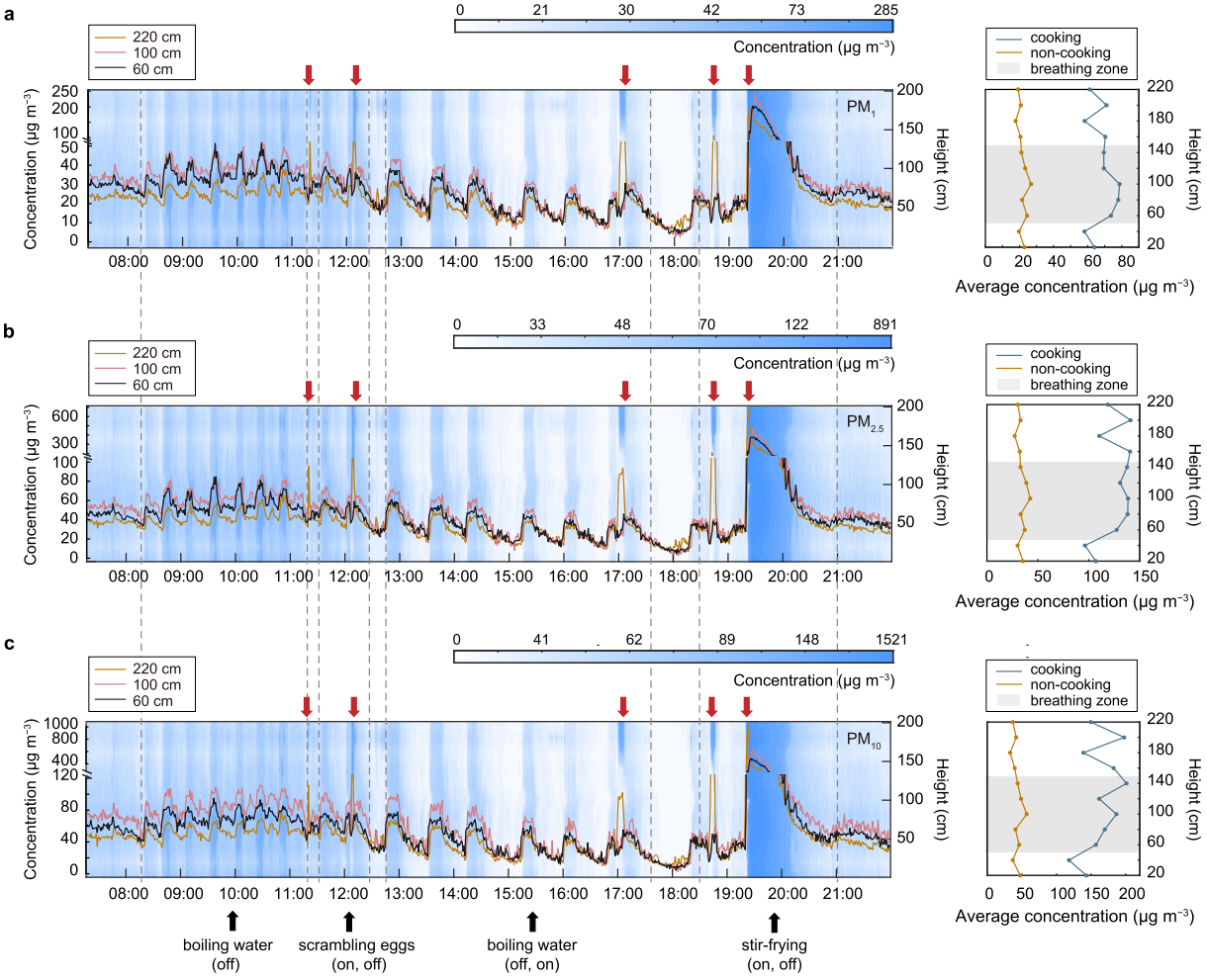


**Fig. 3.** Temporal and vertical variations in indoor PM during the campaign are shown on the left-side panel. **a**, The temporal (left) and vertical (right) variations of $PM_1$. **b**, The temporal (left) and vertical (right) variations of $PM_{2.5}$. **c**, The temporal (left) and vertical (right) variations of $PM_{10}$. The heights are shown on the right-y-axis. The darker the blue, the higher the concentration, as shown by the color bar above **a**, **b**, and **c**. The yellow, pink, and black lines in the left figure of each panel represent the PM concentrations (shown on the left-y-axis) at 220, 100, and 60 cm, respectively. Five short periods with higher upper-layer PM were marked by red arrows. Types of cooking events are marked by the black arrows on the bottom of the left-side panel. The vertical profiles of PM concentrations during cooking (blue) and non-cooking (yellow) periods are shown in the far-right figure of each panel. The grey box shape in the far-right figure represents the breathing zone of 0.5–1.5 m. The temporal resolution of the measurement was 1 min. The detection heights of PM were 20, 40, 60, 80, 100, 120, 140, 160, 180, 200, and 220 cm above the floor.

with relatively intense cooking activities (as marked in Fig. 3 by red arrows and shown in Fig. S13 in red lines). A lag-correlation analysis revealed that during all these five cooking events showing higher upper-layer PM (Activities No. 10, 12, 18, 19, and 20), PM variation in the upper layers proceeded those in the middle and lower layers by 2–4 min (Tables S11, S12, and S13) (Supplementary Text S3 for the lag-correlation method), suggesting that PM was carried to upper layers by cooking-induced convection before spreading downward. Such vertical transport dynamics resembled that of gas species. However, the same lag-correlation analysis applied to other events didn't show evident time lags (Tables S14, S15, and S16). Given the highest PM levels found at 80-cm and 100-cm heights during other events, it can be concluded that intense cooking, e.g., stir-frying, pan-frying, or cooking on high heat, tended to shoot PMs to the upper layers, while moderate ones left PMs within the breathing zone.

### 3.3. Temporal trends

Compared to the initial concentrations in the morning when no preparation or cooking activities were conducted, $CO_2$ at both low and high heights were elevated by 22% when two people were preparing in the kitchen, suggesting human metabolism as one of the main sources of indoor $CO_2$ (Table S1). However, there was no elevation in PM during the same period (Table S2). Before the first water-boiling event, we lighted the stove twice. Likely, due to direct leakage from the pipeline, methane rose about 6–10 times at various heights.

During the following six water boiling activities with the kitchen ventilator off, gas and PM species were consistently higher than the background and preparation periods (Tables S1, S2, S17, and S18), indicating the predominant role of natural gas burning in indoor air pollution. It is interesting to note that the heat levels of the stove (low, medium-low, medium, and high) significantly affected $CO_2$ and CO concentrations, both of which increased at higher heat levels, while other gas species or PM didn't have this association (Tables S1 and S2). In the following cooking event—scrambling eggs with the kitchen ventilator off, formaldehyde, TVOCs, and methane further increased by 72.9–257.6%, compared to water boiling, and the increases were detectable at all heights (Fig. 2 and Table S1), which may be associated with oil fumes generated by scrambling eggs (Table S1). PM showed further increases but only at higher heights (Fig. 3 and Table S2). Lower heights, on the other hand, showed a decrease in PM (Fig. 3 and Table S2), compared to water-boiling, which can be attributed to potential stronger convection during scrambling eggs than during boiling water, which convey more PM upward. Turning on the ventilator substantially reduced the gas species produced during scrambling eggs, especially at higher heights. For example, the concentration of $CO_2$ and the other four species at 199 cm were reduced by 57% and 72–87%, respectively (Fig. S10). Like the gas species, turning on the ventilator reduced the PM concentrations at heights above 160 cm by more than 40%. However, PM concentrations below 140 cm were not reduced (Fig. S12).

The concentrations of PM during the last event were much higher than those during other events (e.g., boiling water, heating garlic sprouts, and scrambling eggs) (Fig. 3). The mean concentrations in the medium and lower layers (100 and 60 cm) were at least four times higher than other events, and those in the upper layer (220 cm) were at least three times higher. Additionally, turning on the ventilator could substantially reduce the concentrations of gas species and PM at all heights (Fig. S11 and Fig. S13). For example, PM concentrations below 160 cm were reduced by more than 80% with the ventilator on, and the concentrations of gas species above 119 cm were reduced by at least 55%. Gas species did not show significantly higher concentrations during this event (Fig. 2 and Table S1). Given that we kept the window closed and the kitchen ventilators off during and after the last cooking activity (i.e., stir-frying the cabbage after pan-frying the pepper and onion), it took about 2 h for the concentrations of gas species to decrease by 70%, equivalent to a half-life of approximately 1.8 h ($t_{1/2}$, i.e., the time for the concentration to reduce by half of its peak). In contrast, $t_{1/2}$ of the three PM sizes were all less than 30 min, likely due to a faster loss via direct indoor deposition than gas species. Among the three PM sizes, $PM_{10}$ declined at the fastest pace ($t_{1/2} = 17$ min), followed by $PM_{2.5}$ ($t_{1/2} = 21$ min) and then $PM_1$ ($t_{1/2} = 28$ min), suggesting that larger particles are subject to rapid removal through direct deposition in indoor environments and smaller particles which are more harmful to human health can suspend indoors for a longer time. The result is consistent with the conclusion reported by You et al. that the particle deposition velocities approximately linearly increased with particle size in indoor environments (1–10 μm) [48].

We employed the concentrations during the non-cooking periods (shown in Fig. 3b) to estimate the overall background concentration of $PM_{2.5}$. The time series of background $PM_{2.5}$ averaged over the three representative heights (60, 100, and 200 cm) showed a sine-like shape and was correlated with outdoor $PM_{2.5}$ concentrations ($r = 0.64$, $p = 0.018$) (Figs. S8 and S9), indicating that outdoor-to-indoor infiltration was also an important source of indoor PM pollution. In this case, the background concentrations during every cooking activity may vary with outdoor concentrations. We thus employed the concentrations of two consecutive non-cooking periods as the background concentration of specific cooking activity and calculated the cooking-induced increase rate of each cooking activity separately based on the background concentration. We found that cooking activities increased indoor levels of gas species by 21–106% and PM by 44–159% (as the interquartile range) compared to the corresponding background concentrations (Tables S17 and S18). The concentrations of five gas species were comparable to those of the same gas species detected in a previous study during Chinese cooking on a natural gas stove [3]. And the cooking-induced PM levels during the experiments were close to those reported in a previous study where PM concentrations were measured during Chinese cooking on natural gas stoves in 25 residential buildings [49]. However, it should be noted that the measurements were only conducted in one kitchen. Although the kitchen has a typical layout constrained by design standards and following common styles, more measurements in multiple kitchens are needed to evaluate the robustness of the results presented here.

## 4. Implications

In China, the urban population accounted for 63.89% of the total population in 2021, and the proportion is still rising in the content of urbanization [50]. The impact of urban household cooking on overall population exposure will arguably become increasingly broader than that of rural household cooking. Several studies have shown that exposure to high levels of air pollutants for hours or even several minutes can be associated with acute health effects [44,51–54]. For example, short-term exposure to high particulate matter concentration was associated with acute airway inflammation and impaired lung function [51]. In this study, we found that cooking activities caused concentration spikes, significantly increasing indoor levels of gas species by 21–106% and PM by 44–159% in the kitchen for a short term. The increased indoor air pollution during cooking thus has potential acute health consequences, especially for those who cook (due to direct exposure to the pollutants released by cooking). Given the cooking-induced pollution elevation and the evidence linking short-term exposure to adverse health effects, the impacts of cooking on the health of

occupants warrant further investigation.

Our campaign considered various factors (e.g., cooking time, ventilation condition, cooking technique, temperature, ingredient, etc.) that affect the magnitude of the short-term pollution elevation during cooking. For example, we found that several typical Chinese cooking styles, such as pan-frying and stir-frying, tended to produce extra amounts of PM while also tolerating the vertical profiles due to the high cooking intensity. The level of exposure to air pollutants during cooking will depend on the height of the individual who cooks and what type of cooking is conducted. The results are likely instrumental in forming good cooking practices that benefit population health from the perspective of household air pollution.

The monitoring technical guideline of the indoor air quality standard in China does not have a prescribed sampling height but recommends any height within the "breathing zone" to conduct the indoor measurements, assuming that the concentration within the breathing zone is uniform [35]. Here, we represent the first investigation of the vertical profiles of indoor pollutants during cooking. The results revealed substantial vertical variation even within the breathing zone. The high vertical variability challenges the current guideline and suggests that vertical information should be considered in forming indoor air quality standards in the next version.

## 5. Conclusions

In this study, we used highly temporally resolved low-cost sensors to measure five gas species and PM at multiple heights in a kitchen during Chinese cooking. We found indoor gas species were elevated by 21%–106% during cooking, compared to the background, and PMs were elevated by 44%–159%. Vertically, the pollutants concentrations were highly variable. Gas species generally showed a monotonic increase with height, while PMs changed more diversely depending on the intensity of the cooking activities. Intense cooking, e.g., stir-frying, pan-frying, or cooking on high heat, tended to shoot PMs to the upper layers, while moderate ones left PMs within the breathing zone. Considering the health implications, we call attention to the high vertical variability of air pollution in indoor micro-environments that the science community and policymakers have so far overlooked. The short spikes and the high vertical variability of indoor air pollution during cooking have important health implications but have been so far overlooked by the science community and policymakers. Further investigation is needed to acquire instrumental information on the temporal and vertical variation in indoor air quality and helps form specific standards and policies that reduce short-term indoor air pollution exposure induced by cooking.

## Declaration of interests

The authors declare that they have no known competing financial interests or personal relationships that could have appeared to influence the work reported in this paper.

## Acknowledgments

This research is supported by the National Natural Science Foundation of China (Grants 41991312, 41821005, 41922057, 41830641, and 42192510), Shenzhen Environmental Monitoring Center (Grant 0722-216FE4812SZF-2), Department of Education of Guangdong Province (2021KCXTD004), and Center for Computational Science and Engineering at Southern University of Science and Technology.

## Supporting information

Supplementary materials include the correction method and coefficient of the concentrations of five gas species and PM, the lag-correction method, the analysis and variance method, the layout of the indoor monitoring campaign, the histogram, skewness and kurtosis, and Lilliefors test for five gas species and PM, the concentrations of $CO_2$ at different heights during Activity No. 12, the Student-Newman-Keuls multi-comparison of PM during cooking events and non-cooking period, the outdoor concentrations of $PM_{2.5}$, the background concentrations of $PM_{2.5}$, the concentrations of five gas species and PM during Act. No. 11 and Act. No. 12, the concentrations of five gas species and PM during Act. No. 19 and Act. No. 20, the vertical profiles of PM in three sizes during all cooking events, the probability density distributions of PM, the concentrations of five gas species and PM during each cooking activity, one-sample T-test of the ratios of concentrations at 199 cm to those at 78 cm for gas species during cooking and non-cooking period, lag-correlation coefficients of PM between 80 cm and the other ten heights during the intense cooking events (Activities No. 10, 12, 18, 19, and 20) and the other cooking events, the average concentrations of five gas species at different heights during cooking and non-cooking periods, the correlation coefficient of the gas concentrations at 78-cm height with the concentrations at the other five heights and the measured parameters of the photo-acoustic gas monitor.

## Appendix A. Supplementary data

Supplementary data to this article can be found online at https://doi.org/10.1016/j.ese.2022.100200.

## References

[1] S.C. Lee, W.M. Li, C.H. Ao, Investigation of indoor air quality at residential homes in Hong Kong - case study, Atmos. Environ. 36 (2) (2002) 225–237.
[2] Z. Shao, J. Bi, Z. Ma, J. Wang, Seasonal trends of indoor fine particulate matter and its determinants in urban residences in Nanjing, China, Build. Environ. 125 (2017) 319–325.
[3] G. Shen, S. Ainiwaer, Y. Zhu, S. Zheng, W. Hou, H. Shen, Y. Chen, X. Wang, H. Cheng, S. Tao, Quantifying source contributions for indoor CO2 and gas pollutants based on the highly resolved sensor data, Environ. Pollut. (2020) 267.
[4] H.Z. Shen, W.Y. Hou, Y.Q. Zhu, S.X. Zheng, S. Ainiwaer, G.F. Shen, Y.L. Chen, H.F. Cheng, J.Y. Hu, Y. Wan, S. Tao, Temporal and spatial variation of PM2.5 in indoor air monitored by low-cost sensors, Sci. Total Environ. (2021) 770.
[5] S. Archer-Nicholls, E. Carter, R. Kumar, Q. Xiao, Y. Liu, J. Frostad, M.H. Forouzanfar, A. Cohen, M. Brauer, J. Baumgartner, C. Wiedinmyer, The regional impacts of cooking and heating emissions on ambient air quality and disease burden in China, Environ. Sci. Technol. 50 (17) (2016) 9416–9423.
[6] WHO, Global burden of disease, Website, https://vizhub.healthdata.org/gbd-compare/.
[7] Y. Hu, B. Zhao, Indoor sources strongly contribute to exposure of Chinese urban residents to PM2.5 and NO2, J. Hazard Mater. 426 (2022), 127829.
[8] M. Qi, W. Du, X. Zhu, W. Wang, C.X. Lu, Y.C. Chen, G.F. Shen, H.F. Cheng, E.Y. Zeng, S. Tao, Fluctuation in time-resolved PM2.5 from rural households with solid fuel-associated internal emission sources, Environ. Pollut. 244 (2019) 304–313.
[9] W. Du, X.Y. Li, Y.C. Chen, G.F. Shen, Household air pollution and personal exposure to air pollutants in rural China - a review, Environ. Pollut. 237 (2018) 625–638.
[10] S. Tao, M.Y. Ru, W. Du, X. Zhu, Q.R. Zhong, B.G. Li, G.F. Shen, X.L. Pan, W.J. Meng, Y.L. Chen, H.Z. Shen, N. Lin, S. Su, S.J. Zhuo, T.B. Huang, Y. Xu, X. Yun, J.F. Liu, X.L. Wang, W.X. Liu, H.F. Cheng, D.Q. Zhu, Quantifying the rural residential energy transition in China from 1992 to 2012 through a representative national survey, Nat. Energy 3 (7) (2018) 567–573.
[11] S. Bonjour, H. Adair-Rohani, J. Wolf, N.G. Bruce, S. Mehta, A. Pruss-Ustun, M. Lahiff, E.A. Rehfuess, V. Mishra, K.R. Smith, Solid fuel use for household cooking: country and regional estimates for 1980-2010, Environ. Health Persp. 121 (7) (2013) 784–790.
[12] H.M. Xu, Y.Q. Li, B. Guinot, J.H. Wang, K.L. He, K.F. Ho, J.J. Cao, Z.X. Shen, J. Sun, Y.L. Lei, X.S. Gong, T. Zhang, Personal exposure of PM2.5 emitted from solid fuels combustion for household heating and cooking in rural Guanzhong Plain, northwestern China, Atmos. Environ. 185 (2018) 196–206.

[13] Z.A. Chafe, M. Brauer, Z. Klimont, R. Van Dingenen, S. Mehta, S. Rao, K. Riahi, F. Dentener, K.R. Smith, Household cooking with solid fuels contributes to ambient PM2.5 air pollution and the burden of disease, Environ. Health Perspect. 122 (12) (2014) 1314–1320.
[14] H. Shen, Z. Luo, R. Xiong, X. Liu, L. Zhang, Y. Li, W. Du, Y. Chen, H. Cheng, G. Shen, S. Tao, A critical review of pollutant emission factors from fuel combustion in home stoves, Environ. Int. 157 (2021), 106841.
[15] China Academic Journal Electronic Publishing House, Almanac of China's Population. (C)1994-2021(in Chinese).
[16] X.Y. Zheng, C. Wei, P. Qin, J. Guo, Y.H. Yu, F. Song, Z.M. Chen, Characteristics of residential energy consumption in China: findings from a household survey, Energy Pol. 75 (2014) 126–135.
[17] Special market research and investment prospect research report of China's urban gas industry (2022-2028) (in Chinese), https://www.chyxx.com/research/202110/978614.html.
[18] US EPA, Natural gas combustion. https://www3.epa.gov/ttnchie1/ap42/ch01/final/c01s04.pdf.
[19] J.M. Logue, N.E. Klepeis, A.B. Lobscheid, B.C. Singer, Pollutant exposures from natural gas cooking burners: a simulation-based assessment for Southern California, Environ. Health Perspect. 122 (1) (2014) 43–50.
[20] S.A. Ardeh, S.S. Khaloo, R. Gholamnia, M. Abtahi, R. Saeedi, Assessment of indoor air pollutant concentrations and emissions from natural gas cooking burners in residential buildings in Tehran, Iran, Air. Qual. Atmos. Hlth. 13 (4) (2020) 409–420.
[21] Z. Merrin, P.W. Francisco, Unburned methane emissions from residential natural gas appliances, Environ. Sci. Technol. 53 (9) (2019) 5473–5482.
[22] C.H. Lai, J.J. Jaakkola, C.Y. Chuang, S.H. Liou, S.C. Lung, C.H. Loh, D.S. Yu, P.T. Strickland, Exposure to cooking oil fumes and oxidative damages: a longitudinal study in Chinese military cooks, J. Expo. Sci. Environ. Epidemiol. 23 (1) (2013) 94–100.
[23] G. Buonanno, L. Morawska, L. Stabile, Particle emission factors during cooking activities, Atmos. Environ. 43 (20) (2009) 3235–3242.
[24] Y. Zhao, M. Hu, S. Slanina, Y. Zhang, The molecular distribution of fine particulate organic matter emitted from Western-style fast food cooking, Atmos. Environ. 41 (37) (2007) 8163–8171.
[25] L.A. Wallace, S.J. Emmerich, C. Howard-Reed, Source strengths of ultrafine and fine particles due to cooking with a gas stove, Environ. Sci. Technol. 38 (8) (2004) 2304–2311.
[26] Q.F. Zhang, R.H. Gangupomu, D. Ramirez, Y.F. Zhu, Measurement of ultrafine particles and other air pollutants emitted by cooking activities, Int. J. Environ. Res. Publ. Health 7 (4) (2010) 1744–1759.
[27] S.W. See, R. Balasubramanian, Risk assessment of exposure to indoor aerosols associated with Chinese cooking, Environ. Res. 102 (2) (2006) 197–204.
[28] Y.J. Zhao, B. Zhao, Emissions of air pollutants from Chinese cooking: a literature review, Build. Simul. China 11 (5) (2018) 977–995.
[29] M.P. Wan, C.L. Wu, G.N. Szeto, T.C. Chan, C.Y.H. Chao, Ultrafine particles, and PM2.5 generated from cooking in homes, Atmos. Environ. 45 (34) (2011) 6141–6148.
[30] Y.J. Zhao, A.G. Li, R. Gao, P.F. Tao, J. Shen, Measurement of temperature, relative humidity and concentrations of CO, CO2 and TVOC during cooking typical Chinese dishes, Energy Build. 69 (2014) 544–561.
[31] Z.-H. Huang, S.-C. Li, D.-X. Yu, H. Qiu, X.-L. Huang, Investigation on environment of Chinese restaurants in Hong Kong, Chin. J. Ind. Hyg. Occup. Dis. 26 (8) (2008) 474–476 (in Chinese).
[32] C.M. Liao, S.C. Chen, J.W. Chen, H.M. Liang, Contributions of Chinese-style cooking and incense burning to personal exposure and residential PM concentrations in Taiwan region, Sci. Total Environ. 358 (1–3) (2006) 72–84.
[33] M. Dennekamp, S. Howarth, C.A.J. Dick, J.W. Cherrie, K. Donaldson, A. Seaton, Ultrafine particles and nitrogen oxides generated by gas and electric cooking, Occup. Environ. Med. 58 (8) (2001) 511–516.
[34] L.N. Wang, L.Y. Zhang, Z. Ristovski, X.R. Zheng, H.L. Wang, L. Li, J. Gao, F. Salimi, Y.Q. Gao, S.G. Jing, L. Wang, J.M. Chen, S. Stevanovic, Assessing the effect of reactive oxygen species and volatile organic compound profiles coming from certain types of Chinese cooking on the toxicity of human bronchial epithelial cells, Environ. Sci. Technol. 54 (14) (2020) 8868–8877.
[35] General Administration of Quality Supervision, Inspection and Quarantine, Indoor Air Quality Standard GB/T 18883-2202, 2002 (in Chinese).
[36] Y. Qiu, S. Tao, X. Yun, W. Du, G. Shen, C. Lu, X. Yu, H. Cheng, J. Ma, B. Xue, J. Tao, J. Dai, Q. Ge, Indoor PM2.5 profiling with a novel side-scatter indoor lidar, Environ. Sci. Technol. Lett. 6 (10) (2019) 612–616.
[37] A. Micallef, J. Caldwell, J.J. Colls, The influence of human activity on the vertical distribution of airborne particle concentration in confined environments: preliminary results, Indoor Air 8 (2) (1998) 131–136.
[38] A. Micallef, J.J. Colls, J. Caldwell, Measurement of vertical concentration profiles of airborne particulate matter in indoor environments: implications for refinement of models and monitoring campaigns, Int. J. Environ. Health Res. 9 (1) (1999) 5–18.
[39] A. Micallef, C.N. Deuchar, J.J. Colls, Indoor and outdoor measurements of vertical concentration profiles of airborne particulate matter, Sci. Total Environ. 215 (3) (1998) 209–216.
[40] W. Gao, D.D. Cao, K. Lv, J. Wu, Y.J. Wang, C. Wang, Y.W. Wang, G.B. Jiang, Elimination of short-chain chlorinated paraffins in diet after Chinese traditional cooking-a cooking case study, Environ. Int. 122 (2019) 340–345.
[41] S. Palzer, Photoacoustic-based gas sensing: a review, Sensors-Basel 20 (9) (2020).
[42] C.X. Lu, H.R. Xu, W.J. Meng, W.Y. Hou, W.X. Zhang, G.F. Shen, H.F. Cheng, X.J. Wang, X.L. Wang, S. Tao, A novel model for regional indoor $PM_{2.5}$ quantification with both external and internal contributions included, Environ. Int. (2020) 145.
[43] https://www.rstudio.com.
[44] WHO, WHO guidelines for indoor air quality: selected pollutants. https://www.who.int/publications/i/item/9789289002134.
[45] Kernel density estimation, matthew conlen. https://mathisonian.github.io/kde/.
[46] Ministry of Ecology and Environment of the People's Republic of China, Ambient Air Quality Standard GB 3095-2012 (in Chinese).
[47] WHO IAQ standards and guidelines. https://foobot.io/guides/iaq-standards-and-guidelines.php.
[48] R.Y. You, B. Zhao, C. Chen, Developing an empirical equation for modeling particle deposition velocity onto inclined surfaces in indoor environments, Aerosol Sci. Technol. 46 (10) (2012) 1090–1099.
[49] K. Kang, H. Kim, D.D. Kim, Y.G. Lee, T. Kim, Characteristics of cooking-generated $PM_{10}$ and $PM_{2.5}$ in residential buildings with different cooking and ventilation types, Sci. Total Environ. 668 (2019) 56–66.
[50] Bureau of Statistics, PRC, Bulletin of the seventh national census (in Chinese) (No. 7), http://www.stats.gov.cn/xxgk/sjfb/zxfb2020/202105/t20210511_1817202.html, 2021, 410A04-410402-202105-0005.
[51] M. Strak, N.A.H. Janssen, K.J. Godri, I. Gosens, I.S. Mudway, F.R. Cassee, E. Lebret, F.J. Kelly, R.M. Harrison, B. Brunekreef, M. Steenhof, G. Hoek, Respiratory health effects of airborne particulate matter: the role of particle size, composition, and oxidative potential-the RAPTES project, Environ. Health Persp. 120 (8) (2012) 1183–1189.
[52] J.A. Dye, J.R. Lehmann, J.K. McGee, D.W. Winsett, A.D. Ledbetter, J.I. Everitt, A.J. Ghio, D.L. Costa, Acute pulmonary toxicity of particulate matter filter extracts in rats: coherence with epidemiologic studies in Utah Valley residents, Environ. Health Persp. 109 (2001) 395–403.
[53] L.L. Yu, B. Wang, M. Cheng, M. Yang, S.M. Gan, L.Y. Fan, D.M. Wang, W.H. Chen, Association between indoor formaldehyde exposure and asthma: a systematic review and meta-analysis of observational studies, Indoor Air 30 (4) (2020) 682–690.
[54] K. Azuma, N. Kagi, U. Yanagi, H. Osawa, Effects of low-level inhalation exposure to carbon dioxide in indoor environments: a short review on human health and psychomotor performance, Environ. Int. 121 (2018) 51–56.